AGU PUBLICATIONS

JGR

Journal of Geophysical Research: Biogeosciences

RESEARCH ARTICLE
10.1002/2017JG003871

Key Points:
- Temperature effects on coastal nitrification rates are significant in all seasons
- A consistent Q_{10} value of ~2.2 was obtained regardless of distinctive seasonal temperature and particulate concentrations
- Particles are important in regulation of coastal nitrification rates

Supporting Information:
- Supporting Information S1
- Figure S1

Correspondence to:
S.-J. Kao,
sjkao@xmu.edu.cn

Citation:
Zheng, Z.-Z., X. Wan, M. N. Xu, S. S.-Y. Hsiao, Y. Zhang, L.-W. Zheng, Y. Wu, W. Zou, and S.-J. Kao (2017), Effects of temperature and particles on nitrification in a eutrophic coastal bay in southern China, *J. Geophys. Res. Biogeosci.*, *122*, 2325–2337, doi:10.1002/2017JG003871.

Received 8 APR 2017
Accepted 11 AUG 2017
Accepted article online 21 AUG 2017
Published online 11 SEP 2017

Effects of temperature and particles on nitrification in a eutrophic coastal bay in southern China

Zhen-Zhen Zheng[1], Xianhui Wan[1], Min Nina Xu[1], Silver Sung-Yun Hsiao[2], Yao Zhang[1], Li-Wei Zheng[1], Yanhua Wu[3], Wenbin Zou[1], and Shuh-Ji Kao[1]

[1]State Key Laboratory of Marine Environmental Science, College of Ocean and Earth Sciences, Xiamen University, Xiamen, China, [2]Research Center for Environmental Changes, Academia Sinica, Taipei, Taiwan, [3]Shenzhen Marine Environment Monitoring Center Station, State Oceanic Administration, Shenzhen, China

Abstract Despite being the only link between reduced and oxidized nitrogen, the impact of environmental factors on nitrification, temperature and particles, in particular, remains unclear for coastal zones. By using the $^{15}NH_4^+$-labeling technique, we determined nitrification rates in bulk (NTR_B) and free-living (NTR_F, after removing particles >3 μm) for water samples with varying particle concentrations (as sampled at different tidal stages) during autumn, winter, and summer in a eutrophic coastal bay in southern China. The highest NTR_B occurred in autumn, when particle concentrations were highest. In general, particle-associated nitrification rates (NTR_P, >3 μm) were higher than NTR_F and increased with particle abundance. Regardless of seasonally distinctive temperature and particle concentrations, nitrification exhibited consistent temperature dependence in all cases (including bulk, particle-associated, and free-living) with a Q_{10} value of ~2.2. Meanwhile, the optimum temperature for NTR_P was ~29°C, 5°C higher than that for NTR_F although the causes for such a difference remained unclear. Strong temperature dependence and particle association suggest that nitrification is sensitive to temperature change (seasonality and global warming) and to ocean dynamics (wave and tide). Our results can potentially be applied to biogeochemical models of the nitrogen cycle for future predictions.

1. Introduction

The global nitrogen cycle has been altered significantly due to the continuously growing input of anthropogenic nitrogen [*Gruber and Galloway*, 2008; *Yang and Gruber*, 2016], and this has been suggested to be the most serious ecological problem, second only to biodiversity loss [*Rockström et al*., 2009]. The impacts of cumulative input of anthropogenic nitrogen from atmospheric and riverine systems were evident on nitrogen and phosphorous stoichiometry in surface waters in marginal seas and even in subsurface layers in the North Pacific [*Kim et al*., 2014; *Wong et al*., 1998]. Nitrification, one of the better-known nitrogen processes, oxidizes ammonia into nitrate, connecting reduced and oxidized inorganic nitrogen pools and playing a critical role in the marine nitrogen cycle. Nitrification also links to global warming as it involves the production of nitrous oxide (N_2O) [*Santoro et al*., 2011], which carries a 300-fold higher greenhouse gas potential than carbon dioxide. In addition, nitrification enhances acidification and promotes hypoxia in estuary and river plume systems by reducing alkalinity [*Hu and Cai*, 2011] and consuming oxygen, respectively [*Dai et al*., 2008; *Grundle and Juniper*, 2011]. Therefore, in coastal zones where anthropogenic nitrogen loads (including ammonium, nitrate, and organic nitrogen) are high, nitrification associated environmental issues is severe. Despite this importance, information on environmental factors that control nitrification rates (NTRs) in hydrodynamically active coastal seas is limited.

Environmental factors, such as ammonium, suspended sediment, temperature, salinity, pH, oxygen, and light, may regulate NTR in aquatic environments [*Ward*, 2008; *Beman et al*., 2012; *Isnansetyo et al*., 2014]. Results from the inventory method coupled with inhibition suggest temperature may serve as the most important environmental factor in substrate-replete coastal seas [*Berounsky and Nixon*, 1990; *Dai et al*., 2008]. However, field experiments on nitrification temperature dependence have been limited, and the most relevant data to date were derived from pure cultures [*Groeneweg et al*., 1994; *Qin et al*., 2014], fixed-bed reactors in wastewater treatment plants [*Sudarno et al*., 2011], and nonmarine environments such as soils [*Tourna et al*., 2008], rivers [*Stratton and McCarty*, 1967], freshwater sediments [*Wu et al*., 2013], and intertidal zones [*Isnansetyo et al*., 2014]. In contrast, available marine data, such as those from the Hood Canal and the western coastal Arctic, suggested that NTRs are not temperature dependent [*Horak et al*., 2013; *Baer et al*., 2014]. The

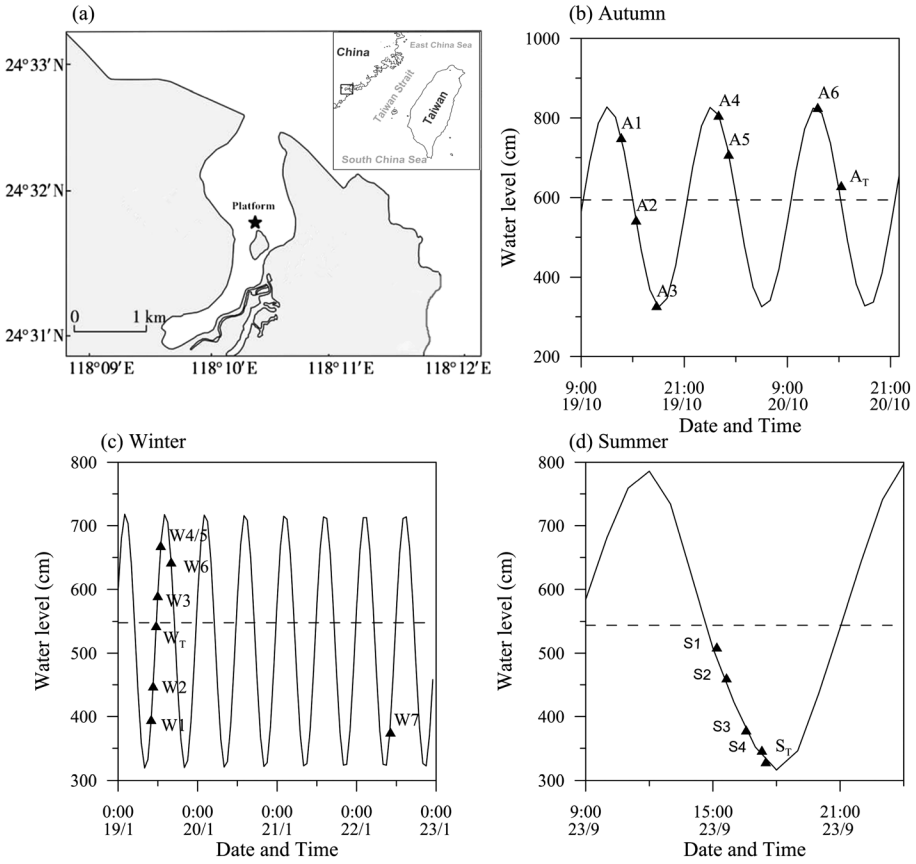

Figure 1. (a) Location of Wuyuanwan Bay at the southern coast of China (24°31′48″N, 118°10′47″E). Tidal curves (solid lines) and sampling times (black triangles) for (b) autumn, (c) winter, and (d) summer. Dashed lines represent mean water depths over the sampling period.

lack of significant influence of temperature upon marine NTR had been attributed to a combination of other environmental factors [*Ward*, 2008]. Thus, the nitrification response to temperature changes remains ambiguous. Besides temperature, previous reports in coastal seas have indicated that nitrifiers have high affinity toward particles [*Xia et al*., 2009; *Wang et al*., 2010; *Füssel et al*., 2012; *Hsiao et al*., 2014; *Zhang et al*., 2014], but particle-associated nitrification rates results are limited and the correlations between suspended particle and NTR are not well understood.

Due to the rapidly growing population in China, intensive human activities, including the development of coastal cities, effluent discharges from upstream agriculture, aquaculture, and animal farming lands, have increased riverine nutrient loads up to ~10 times over recent decades [*Dai et al*., 2010; *Yan et al*., 2012]. Similar nitrogen load increments have been widely reported in many large river basins in the world [e.g., *García-Serna et al*., 2013]. In China, huge suspended sediment inputs accompany these nutrient loads, endowing coastal systems with a distinctive feature of high turbidity. In summer high river flow periods, turbid coastal waters in Chinese coastal seas can often be seen in satellite images [e.g., *Hsiao et al*., 2014, Figure 1]. While in winter time, vigorous hydrodynamics driven by the prevailing monsoon winds also generate high levels of resuspension.

Under the 2013 Intergovernmental Panel on Climate Change Representative Concentration Pathways (RCP) 2.6 and RCP 8.5 scenarios [*Collins et al*., 2013], the global sea surface temperature will increase by 0.4–4°C by 2100. Furthermore, various atmosphere-ocean coupling models suggest that Chinese marginal seas will experience the most significant sea surface temperature increases in the entire North Pacific region [*Deser et al*., 2010]. Coupled with the seasonal flood input and year-round resuspension, Chinese coastal seas provide a great opportunity to explore the relationships between nitrification and environmental factors, especially the roles of turbidity and temperature. In this study, the often used ^{15}N-tracer technique

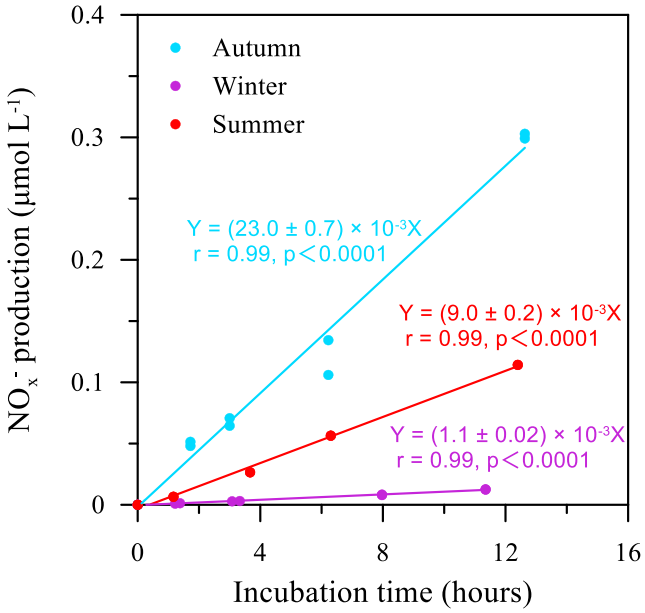

Figure 2. NO_x^- productions over the incubation time for autumn, winter, and summer cases.

[*Lipschultz et al.*, 1986; *Ward*, 2005] was applied to quantify the effect of temperature and particles on nitrification in a eutrophic coastal bay in southern China, which is representative of Chinese coastal seas.

2. Materials and Methods

2.1. Sampling

As shown in Figure 1, water samples with varying temperatures and particle concentrations (as a result of different tidal stages) were collected in three field trips during 19–20 October 2013 (autumn), 19–23 January 2014 (winter), and on 23 September 2014 (end of summer) from a floating platform in Wuyuanwan Bay in southern China (24°31′48″ N, 118°10′47″E). To enable temperature manipulation experiments, we collected 18 L of water in total.

2.2. Chemical Analyses

Salinity and temperature were measured with a conductivity-temperature-depth profiler. Ammonium was analyzed via the indophenol blue spectrophotometric method with a detection limit of 0.3 μmol L^{-1} [*Pai et al.*, 2001]. Nitrite plus nitrate (NO_x^-) was measured using the chemiluminescent technique [*Braman and Hendrix*, 1989] with a 0.01 μmol L^{-1} detection limit. Total suspended sediment (TSS) samples were collected by filtering 1 L through 47 mm precombusted and preweighed glass microfibre filters (GF/F), and weighing after oven drying at 60°C.

2.3. Incubation Experiments

2.3.1. Rate Measurement

For nitrification incubation, we added 0.25 mL of 1 mmol L^{-1} $^{15}NH_4Cl$ (98 atom % ^{15}N; Sigma-Aldrich, 299251-1G, Lot#TA2540V) into 250 mL water samples in narrow-necked brown glass bottles (Qorpak API#2120) to reach a final concentration of 1 μmol L^{-1}. The samples were incubated for 6 h in the dark (in duplicate). Detailed information for this method has been presented in previous studies [*Lipschultz et al.*, 1986; *Newell et al.*, 2011; *Ward*, 2011]. The control samples were filtered immediately (t_0) after tracer addition. To examine the linearity of NO_x^- production within the incubation period, we carried out 12 h incubations with multiple sampling intervals (0, 1, 3, 6 and 12 h) for the experimental set of in situ temperatures (Figure 2). All incubation procedures were terminated by filtering the samples through 0.22 μm polycarbonate membranes, and the filtrate was frozen at −20°C until the laboratory analysis. Whole water was used for the bulk nitrification rate (NTR_B) incubations. Similar procedures were implemented for the incubation of the free-living nitrification rate (NTR_F) after removing particles >3 μm following previous studies [*Watson et al.*, 1981; *Berounsky and Nixon*, 1993]. To reduce cell stress and cell lysis, filtration for the NTR_F incubation was conducted carefully under the pressure of 0.03 Mpa, following previous work [*Shiozaki et al.*, 2009; *Zhang et al.*, 2014]. Moreover, to minimize the retention of free-living microorganisms, we replaced the filter after every ~300 mL, or when the filtration rate reduced significantly. The difference between NTR_B and NTR_F was defined as the particle-associated nitrification rate (NTR_P).

The $\delta^{15}N$ in NO_x^-, the end product of nitrification, was determined using the denitrifier method [*Sigman et al.*, 2001; *Casciotti et al.*, 2002]. Briefly, *Pseudomonas aureofaciens* (ATCC# 13985) was aseptically cultured for 6–10 days. The Griess-Ilosvay method [*Bendschneider and Robinson*, 1952] was used to ensure no residual NO_2^- and to confirm the efficacy of the *Pseudomonas chlororaphis* culture. Then, the denitrifier organisms were concentrated tenfold by centrifugation and split into 3 mL aliquots in 15 mL headspace vials. The

vials were crimp sealed with Teflon-backed silicone septa and purged for 3 h with high purity N_2 to remove the N_2O produced from the nitrate of the culture media and to ensure anaerobic conditions. Samples (10–20 nmol NO_x^-) were then added to the sample vials and were incubated overnight to allow for complete conversion of NO_x^- to N_2O. After the overnight incubation, 0.1 mL of 10 mol L^{-1} sodium hydroxide was added into each sample vial to stop bacterial activity and scavenge CO_2. Subsequently, the isotopic composition of bacterial-produced N_2O was measured using a Gasbench-II (Thermo Fisher) connected to an isotope ratio mass spectrometer (Thermo Delta V Advantage).

In order to obtain accurate $\delta^{15}N$ values, three NO_3^- international reference materials ($\delta^{15}N_{USGS\ 34} = -1.80‰$, $\delta^{15}N_{IAEA\ N3} = 4.70‰$, $\delta^{15}N_{USGS\ 32} = 180.00‰$) were used to calibrate the $\delta^{15}N$-NO_x^- of samples. All calibration curves for this study are presented in Figure S1. The measured $\delta^{15}N$ values were linearly correlated with the reference $\delta^{15}N$ values. Significant linear regressions ($r = 0.9999–1$, $p < 0.0001$), stable slopes (0.97 ± 0.006), and intercepts (1.27 ± 0.43) for multiple standard curves demonstrate our data quality. Moreover, we inserted a laboratory working standard ($\delta^{15}N$ value of 15.0 ± 0.2‰) after every 15–20 samples to affirm the reproducibility of pretreatment and instrument stability.

The nitrification rate was calculated using the following equation:

$$\mathrm{NTR} = \frac{\left(R_{t\ \mathrm{NO}_x^-} - R_{0\ \mathrm{NO}_x^-}\right) \times \left[\mathrm{NO}_x^-\right]}{\mathrm{t}} \times \frac{\left[^{14}\mathrm{NH}_4^+\right] + \left[^{15}\mathrm{NH}_4^+\right]}{\left[^{15}\mathrm{NH}_4^+\right]}, \quad (1)$$

where $R_{t\ NOx-}$ is the atom % ^{15}N in the NO_x^- pool measured at time t, $R_{0\ NOx-}$ is the atom % ^{15}N of initial NO_x pool. $R_{t\ NOx-}$ and $R_{0\ NOx-}$were calculated from the measured $\delta^{15}N{-}NO_x^-$ at time t and at the start of the incubation, respectively. [NO_x^-] is the concentration of the NO_x^- pool measured by the chemiluminescent method. [$^{14}NH_4^+$] and [$^{15}NH_4^+$] are the observed ambient ammonium concentration and the final concentration with the artificial addition of stable isotopic tracer, respectively.

2.3.2. Temperature Manipulation Experiments

To quantify the effects of temperature on NTR, we applied 5–6 temperature treatments ranging from 9 to 34°C with a 5°C interval. The temperatures were maintained by thermostat incubators (± 1°C). The Q_{10} value, which reflects a specific biological rate in response to a temperature increase of 10°C, was calculated.

A simple exponential function, equation (2), is commonly used to adequately describe temperature responses when rates are determined over a range of temperature (below the optimum temperature):

$$\mathrm{NTR} = \mathrm{NTR}_0 e^{kT}, \quad (2)$$

where NTR is the nitrification rate measured at temperature (T), NTR_0 is the nitrification rate at 0°C, and k is a temperature coefficient. The Q_{10} value is then calculated using equation (3):

$$Q_{10} = e^{10k}. \quad (3)$$

3. Results

3.1. Environmental Factors and In Situ Nitrification Rates

Table 1 presents the environmental parameters and in situ NTR for different sampling periods. Distinctive temperatures were observed in autumn (24°C), winter (14°C), and summer (29°C), revealing a prominent seasonality. A narrow range of salinity (29.8–32.4) was found among the seasons, suggesting limited freshwater effects. Within the same sampling periods, temperature and salinity were found to have narrow ranges throughout the bay. By contrast, NH_4^+ and NO_x^- varied within the same sampling date as well as interseasonally. These strong variations were attributable to water exchanges with the inner bay, where nutrients were more abundant. This pattern was evident from the higher concentrations of NH_4^+ and NO_x^- collected during low tide (Table 1). Among the three seasons, winter presented the lowest concentrations of NH_4^+, ranging from 1.1 to 16.8 μmol L^{-1}, while summer presented the lowest NO_x^- values, ranging from 13.3 to 17.6 μmol L^{-1}.

The highest NTR_B was observed in autumn, followed by summer and winter. This seasonal pattern was likely influenced both by TSS and temperature levels. In autumn, NTR_B increased from 278 to 644 nmol L^{-1} d^{-1} as TSS increased from 149 mg L^{-1} to 403 mg L^{-1}. In winter, suspended sediment varied within a narrower and lower range (from 23 to 80 mg L^{-1}) with 1–2 orders of magnitude lower NTR_B (4 to 26 nmol L^{-1} d^{-1}) relative

Table 1. Environmental Factors and In Situ Nitrification Rates for the Sampling Periods[a]

Sample ID	Depth (m)	Temperature (°C)	Salinity (psu)	pH	TSS (mg L^{-1})	NH_4^+ (μmol L^{-1})	NO_x^- (μmol L^{-1})	NTR_B (nmol L^{-1} d^{-1})	NTR_F (nmol L^{-1} d^{-1})
A1	7.1	24.1	31.4	8.18	214	11.0	33.44	428.6 ± 22.1	-
A2	3.6	24.3	31.0	8.17	149	27.0	38.20	278.6 ± 22.1	-
A3	2.9	24.2	31.1	8.18	403	17.6	38.16	644.5 ± 130.9	-
A4	7.2	24.1	31.2	8.17	179	12.6	36.48	381.6 ± 2.8	-
A5	4.3	24.2	30.9	8.15	218	20.4	39.81	359.2 ± 31.2	-
A6	4.6	24.2	31.1	8.17	187	14.0	36.87	319.0 ± 73.8	-
A_T	6.1	24.1	31.5	8.17	338	11.0	38.40	557.0 ± 26.2	-
W1	2.3	13.4	29.9	8.43	50	2.4	32.82	9.8 ± 0.5	0.2 ± 0.0
W2	4.3	13.4	29.8	8.38	52	16.8	36.11	15.3 ± 2.2	2.7 ± 0.7
W3	6.0	13.5	29.8	8.44	77	6.3	34.44	8.5 ± 0.7	1.7 ± 0.2
W4	3.6	13.8	29.9	8.48	64	1.2	24.73	4.3 ± 0.0	1.4 ± 0.2
W5	6.3	13.7	30.2	8.42	80	1.1	26.41	7.5 ± 0.2	0.6 ± 0.2
W6	3.7	13.9	29.9	8.45	67	2.4	31.42	6.0 ± 0.2	1.1 ± 0.2
W7	2.7	13.0	29.9	8.39	46	4.4	26.05	9.9	1.4 ± 0.1
W_T	5.1	13.5	29.9	8.42	23	14.5	33.44	26.4 ± 0.6	11.9 ± 0.4
S1	0.9	29.4	32.3	-	44	18.4	17.55	40.1 ± 0.6	10.8 ± 0.2
S2	2.9	29.2	32.4	-	49	17.4	17.19	200.6 ± 1.4	39.0 ± 0.8
S3	3.0	29.1	32.4	-	50	16.8	16.91	209.5 ± 1.2	42.2 ± 1.5
S4	2.7	29.1	32.4	-	54	15.0	17.13	424.9 ± 33.9	39.1 ± 1.8
S_T	2.5	29.2	32.4	-	85	23.8	13.30	226.0	25.0 ± 1.6

[a]A, W, and S in sample ID represent autumn, winter, and summer, respectively. Subscripts "T" of sample ID indicates these samples were used for temperature manipulation. psu, practical salinity unit.

to autumn. In summer, NTR_B was higher than in winter despite similar TSS levels, apparently promoted by higher temperature.

Free-living nitrification rates ranged from 0.2 to 12 nmol L^{-1} d^{-1}, accounting for 2–35% of NTR_B. NTR_F values were higher in summer, from 11 to 42 nmol L^{-1} d^{-1}, accounting for a slightly higher proportion (9–45% of NTR_B) than in winter. For both winter and summer, the fractional contributions of NTR_F to NTR_B were higher when TSS values were low. Unfortunately, we did not measure NTR_F in autumn, when TSS was the highest. Note that, although the filtration pressure was carefully kept below 0.03 Mpa, some presumably free-living nitrifiers may still be stressed and even lysed, and some may be retained in the >3 μm fraction [*Orsi et al.*, 2015]. Thus, the NTR_F may potentially be underestimated. Although similar treatment to separate particle-associated from free-living bacteria has been used by microbiologists [e.g., *Moeseneder et al.*, 2001; *Zhang et al.*, 2014], caution is still required in the interpretation of this operationally defined separation of particle and free-living contributions to NTR.

3.2. Temperature Manipulation Experiments

In the time series incubations at in situ temperature, a linear increase in NO_x^- production was evident (Figure 2) ($r > 0.9$), suggesting that the dilution effect on ammonium pools (i.e., $^{14}NH_4^+$ replenishment due to remineralization) was insignificant over 12 h of incubation [*Xu et al.*, 2017]. Thus, nitrification rates were derived from the slopes of the linear regressions, and high r values emphasize the reliability of this approach.

In autumn, the average NTR_B at in situ temperature was 557 ± 26 nmol L^{-1} d^{-1}. The NTR_B decreased to approximate 35% of the in situ rate as the temperature decreased from 24°C to 14°C. By contrast, bulk rate increased by 30% as the temperature increased from 24°C to 29°C. However, additional temperature increases (34°C, see Figure 3a) resulted in a reduction of NTR_B that to an even lower rate than the in situ rate. Similar patterns of NTR_B against temperature were found in winter and summer, despite distinctive in situ temperatures in these seasons (Figures 3b and 3c). Meanwhile, an optimum temperature of 29°C for NTR_B was observed for all three seasons.

With respect to NTR_F in winter and summer, we found that (1) free-living nitrification rate was also temperature dependent; (2) the fractional contribution of NTR_F to NTR_B was lower than that of NTR_P, particularly when NTR_B rates were high; and (3) the optimum temperature for NTR_F was 5°C lower (Figures 3b and 3c) than that of NTR_B.

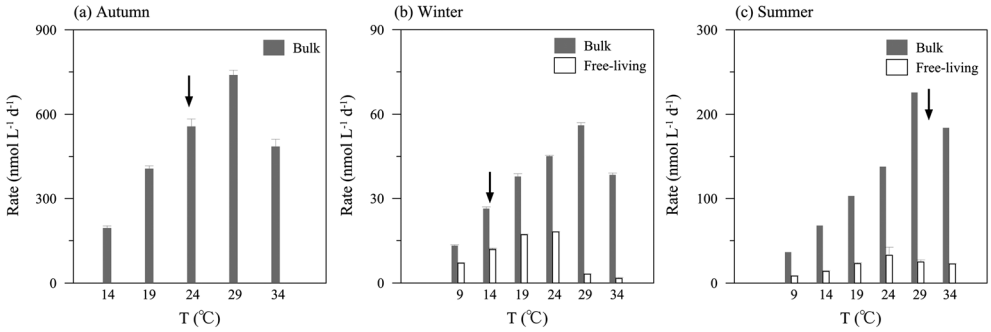

Figure 3. Temperature effects on nitrification rates during (a) autumn, (b) winter, and (c) summer. Arrows denote in situ temperatures. Note that the *y* axis scale differs among the three panels. Error bars denote the standard deviation of duplicates.

4. Discussion

4.1. Temperature Dependence of Nitrification

Although previous studies suggested that seasonal variation of temperature modulates the seasonality of NTR to a considerable degree [*Berounsky and Nixon*, 1990; *Dai et al*., 2008], the specific response of NTR to temperature change in different seasons has not yet been addressed. In our study, since all conditions except temperature remained unchanged, we have the chance to adequately explore the response of NTR specifically to temperature manipulation. Our results showed that below the optimum temperature, NTR increased exponentially as temperature increased in all cases (Figure 4) ($r > 0.9$). This increasing pattern was similar to

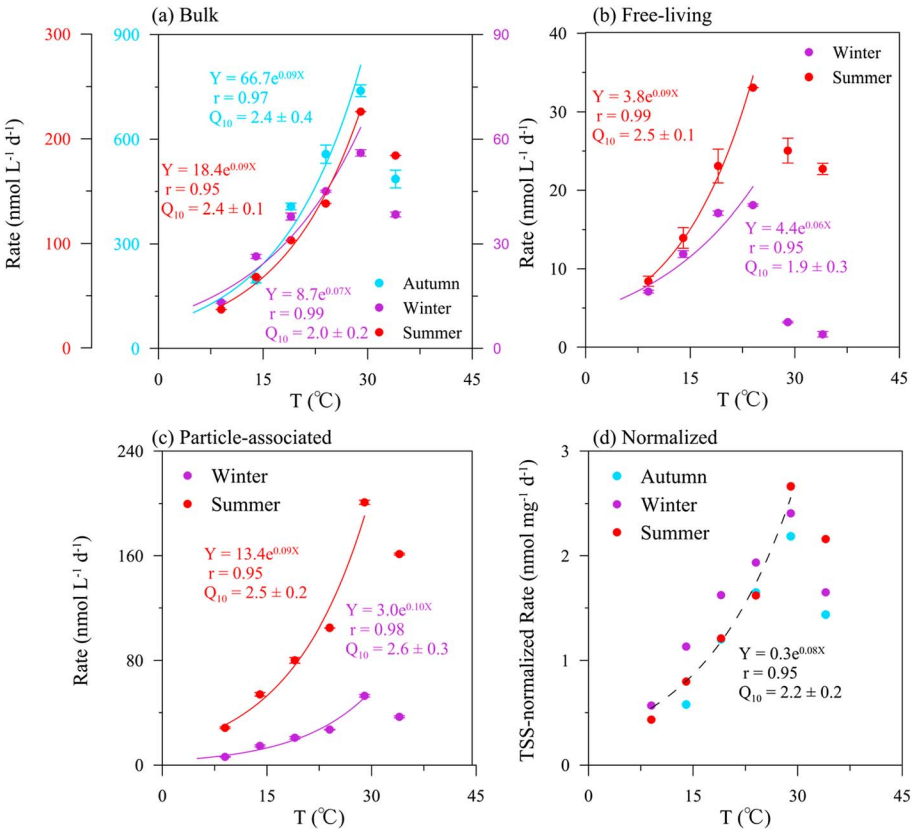

Figure 4. Temperature effects on the nitrification rates of (a) bulk, (b) free-living, (c) particle-associated, and (d) total suspended sediment-normalized samples. Vertical bars represent the standard deviation of duplicates. The color of the regression lines are the same as the data points for each season. The dashed curve in Figure 4d is the regression line of normalized rates for all of the seasons.

the temperature sensitivity of enzyme activity [*Brzostek and Finzi*, 2012]. However, as reviewed in section 1, temperature effects were not found in previous marine studies, perhaps for experimental reasons. For example, the lack of correlation between NTR and temperature in the western coastal Arctic was attributed to the minor responses of microbial communities to short-term warming incubation or to temperature-adaptive capability of high-latitude bacteria, as they function well below their optimum temperature [*Baer et al*., 2014]. The absence of temperature effect in the Hood Canal was attributed to low pH levels or trace metal limitations [*Horak et al*., 2013].

The mean Q_{10} value of bulk (2.2 ± 0.2) was slightly lower than the reported Q_{10} for cultivated ammonia-oxidizing archaea (AOA) (2.89 for *Candidatus Nitrosopumilus maritimus*-SCM1, 2.62 for the Hood Canal station P10-HCA1, and 2.49 for the Puget Sound main basin-PS0) [*Qin et al*., 2014] and was slightly higher than that of the cultivated ammonia-oxidizing bacteria (AOB) (*Nitrosomonas europaea*, Q_{10} = 1.7) [*Groeneweg et al*., 1994]. The field-derived Q_{10} value in our study is likely to provide a more representative temperature sensitivity for nitrifier ensembles in future predictions. Moreover, we found that the Q_{10} values were similar for both NTR_F (2.2 ± 0.2) and NTR_P (2.6 ± 0.2) across the seasons. This is the first field experiment to show indistinguishable temperature dependence for the particle-associated and the free-living nitrification rates. As indicated by *Orsi et al*. [2015], some free-living bacteria (SAR11 and SAR86) may be retained on filters; thus, free-living nitrification rates may potentially be underestimated (and particle-associated rates overestimated). We cannot exclude such a possibility; however, consistent rate responses to temperature were observed for both fractions (Figures 4b and 4c) which may suggest that the current operationally defined method is workable, at least in temperature manipulation experiments.

In addition, the 29°C optimum temperature for bulk rate observed in all temperature manipulation incubations resembles that of pure cultured nitrifying bacteria and that of archaea isolated from temperate environments [*Koops et al*., 2006; *Qin et al*., 2014]. Interestingly, the optimum temperature in our case for NTR_F was 5°C lower though the reasons remain undetermined. Further studies need to be done to resolve this differential optimum temperature issue, which may have implications for prediction the consequences of future ocean warming.

In addition to enzyme activity, the NH_3/NH_4^+ equilibrium is also temperature sensitive [*Johnson et al*., 2008] and has been considered as a potential mechanism for temperature effects. Increased temperature would force the equilibrium toward NH_3, the nitrifier substrate [*Suzuki et al*., 1974; *Ward*, 1987], to stimulate nitrification. In the Wuyuanwan Bay, however, temperature sensitivity of NTR is not likely a result of the NH_3/NH_4^+ equilibrium due to sufficiently high ammonium levels for growth purposes.

Temperature changes may also alter community structure, further affecting rates [*Tourna et al*., 2008; *Feng et al*., 2009; *Bouskill et al*., 2012; *Wu et al*., 2013]. Commonly cultivated strains of AOB (*Nitrosomonas* and *Nitrobacter*) have minimal generation times of 8 h to several days [*Spieck and Bock*, 2005], and AOA (*Candidatus Nitrosopumilus maritimus*-SCM1) have a minimal generation time of 26 h [*Martens-Habbena et al*., 2009]. Both periods are longer than the incubation time applied in our study. Thus, although the community structure may change, it is unlikely that this in the short incubation period could generate the observed exponential temperature dependence. Moreover, the linear increase in NO_x^- production over 12 h (Figure 2) suggested that the rates were constant during the incubations; thus, the effect of community change on NTR could be neglected as indicated previously [*Baer et al*., 2014].

Unlike other estuaries, temperature appears not to modulate the seasonality of NTR in our case (Figure 5d). For instance, the temperature in summer was 5°C higher (under optimum temperature) than autumn, while the in situ rates were lower (Figure 5d). Meanwhile, the temperature manipulation experiments demonstrated a consistent Q_{10} value of ~2.2, which indicated the rate should be doubled with temperature increased by 10°C. However, although the temperature in autumn was 10°C higher than winter, the in situ rates in autumn were more than 1 order magnitude higher than that in winter (Figure 5d), which suggested there are other factors regulating NTR on seasonal scales.

4.2. The Particle Effect on Nitrification

A significant positive linear correlation between NTR_B and TSS was found for the autumn season (r = 0.97, $p < 0.001$) (Figure 5a and Table S1a in the supporting information), probably because particles offer surface area for nitrifier attachment [*Xia et al*., 2009; *Wang et al*., 2010; *Füssel et al*., 2012; *Hsiao et al*., 2014;

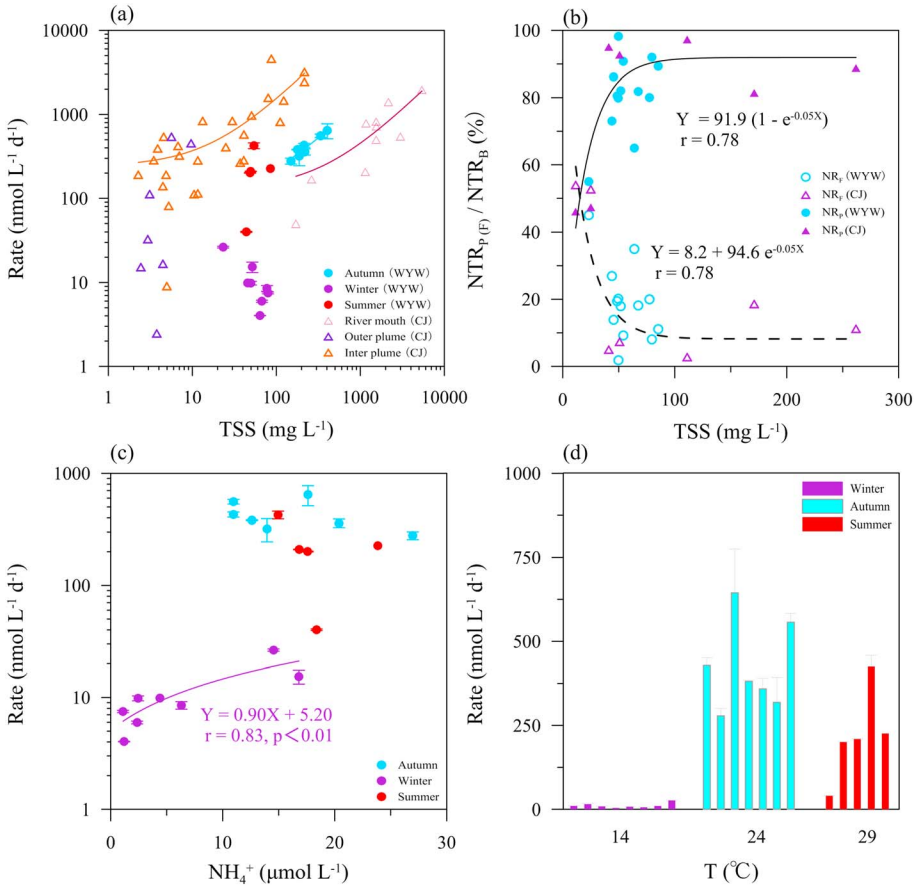

Figure 5. (a) Bulk nitrification rates versus total suspended sediment (TSS) concentrations; Blue (equation $Y = 1.4X + 93$, $r = 0.97$, $p < 0.001$), red, and purple circles represent autumn, summer, and winter data, respectively, of this study. Dark red, orange, and purple open triangles are data from the Changjiang (CJ) River mouth (equation $Y = 0.3X + 127$, $r = 0.84$, $p < 0.05$) and inner (equation $Y = 13X + 238$, $r = 0.75$, $p < 0.001$) and outer river plumes, respectively (data are from *Hsiao et al*. [2014]). (b) Percent contributions of particle associated (solid line) and free-living (dashed line) of bulk nitrification rates against total suspended sediment concentrations (TSS). CJ data are from *Hsiao et al*. [2014]. (c) NTR_B versus ammonium concentrations. (d) Bulk nitrification rates versus temperatures.

Zhang et al., 2014]. Similar positive correlations between NTR_B and TSS have been observed by previous studies in the Changjiang River plume [*Hsiao et al*., 2014], the Seine River [*Brion et al*., 2000], and San Francisco Bay [*Damashek et al*., 2016]. However, no positive relation was found in winter and summer (Tables S1b and S1c), possibly due to the narrow range of TSS variation.

Previously, *Zhang et al*. [2014] found a significant positive relationship between particle-associated *amoA* gene abundance and TSS concentrations in the Changjiang River plume. *Xia et al*. [2009] also observed a power law increase in bacterial populations with the increase of TSS concentrations, which was also accompanied by an increase in NTR. *Wang et al*. [2010] found a significant correlation between the ammonia oxidizing rate and the AOB growth rate, and both rates were enhanced as suspended particles increased. *Wang et al*. [2010] suggested that suspended particles may not only tend to adsorb ammonium but also act as shelters to prevent nitrifiers from light damage. Since the ammonium concentration was replete in our study site, the latter cause is a more likely explanation for our positive correlation.

Our three seasons of data together with results for the Changjiang plume [*Hsiao et al*., 2014] revealed a broad range of NTR_B versus TSS variations (Figure 5a). Significant but distinctive positive correlations between NTR_B and TSS were observed in Changjiang River mouth, Changjiang inner plume, and in autumn in Wuyuanwan Bay. Noteworthily, TSS concentrations on the *x* axis (Figure 5a) are not necessarily equal to the effective surface area, which represents the real habitat size for microorganisms. Therefore, the positive correlation between NTR and TSS is site specific rather than universal, especially in high-energy environments where

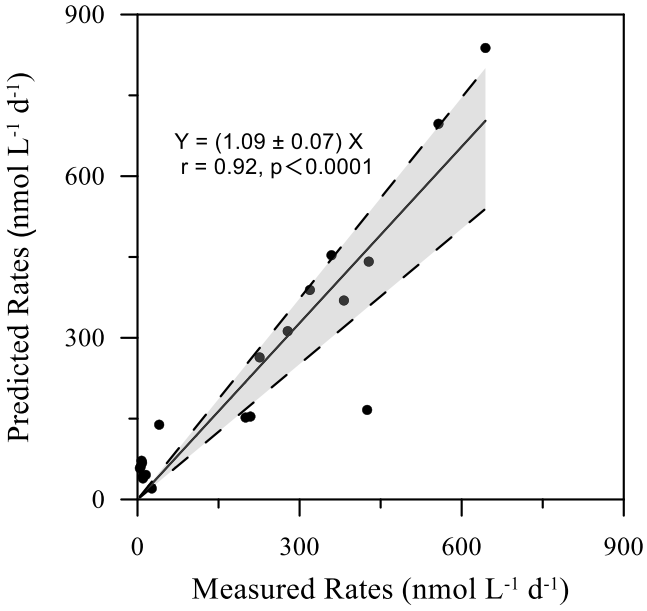

Figure 6. The scatterplot of predicted rates (see text) and measured rates. The dash lines represent the 95% confidence interval.

suspended coarse grains are abundant. Future studies should put more emphasis on the effective surface area of particles for coastal nitrification.

Although nitrifiers have high affinity toward particles [*Xia et al*., 2009; *Wang et al*., 2010; *Füssel et al*., 2012; *Hsiao et al*., 2014; *Zhang et al*., 2014], few studies have partitioned NTR_F and NTR_P. Including consideration of the available Changjiang data reported by *Hsiao et al*. [2014], we found that as the abundance of particles increased, the fraction of total nitrification occurring on particles also increased (Figure 5b). In the coastal system, where the oxygen concentration is high, particle association may help to satisfy the substrate demand for nitrifiers [*Hsiao et al*., 2014; *Wang et al*., 2010] and provide protection against ultraviolet irradiation [*Liltved and Cripps*, 1999]. This may also suggest the importance of nepheloid layer transport in nitrification processes in the South China Sea and other marginal seas. On the contrary, most AOA in the open ocean are free-living due to the low TSS concentration [*Ganesh et al*., 2015; *Peng et al*., 2015, 2016]. According to our results, the contribution of NTR_F to NTR_B increased as TSS concentration decreased (Figure 5b) and the contributions of NTR_F to NTR_B were higher than that of NTR_P when the TSS concentrations were lower than 25 mg L^{-1} (Figure 5b). This is consistent with the dominance of free-living nitrifiers in the open ocean where suspended particle concentrations are well below this level. Alternatively, particle association may not benefit nitrifiers in the oxygen minimum zone (OMZ). For instance, in the OMZ of the eastern tropical North Pacific, *Ganesh et al*. [2015] found most AOA are free-living rather than associated with particles. Distinctive ecology of nitrifiers in oxygenated coastal systems and oxygen minimum zone might be attributable to the oxygen demand of nitrifiers.

The particle effect was also evident in the temperature manipulation experiments. The NTR values increased exponentially with temperature throughout all seasons; however, the highest particle concentrations in autumn occurred in concert with the highest NTR in autumn. We normalized the NTR to TSS to eliminate the particle effect and found that orders of magnitude of variations in NTR across the seasons disappeared (Figure 4d), while a significant exponential relation appeared between TSS-normalized NTR and temperature (Q_{10} = 2.2 ± 0.2, r = 0.95).

This empirical function ($NTR = TSS \times 0.3e^{0.08T}$, Figure 4d) can potentially be used to predict local nitrification once TSS concentrations and water temperature are known. By using this function, we predicted NTR_B values, which fit well with the NTR_B values measured under different tidal levels in different seasons (Figure 6). With this relationship, one can easily predict the instant and annual NTR in the water column of a study area by continuously monitoring the TSS concentrations and temperature (achieving cost savings and high resolution). As mentioned earlier, higher TSS concentrations does not necessarily mean larger effective surface area for microbes; therefore, it is inappropriate to expand this law to other regions where the hydrodynamic setting and particle characteristics may be different. Future work to determine the relationships among NTR, nitrifier biomass, and particle characteristics (especially surface area) is necessary to develop improved predictability of future changes in NTR at larger spatial scales.

4.3. Other Environmental Factors

In addition to temperature and particle concentrations, other environmental factors, e.g., ammonium, salinity, and pH, may influence spatial-temporal variations in nitrification [*Dai et al*., 2008; *Heiss and Fulweiler*, 2016; *Hsiao et al*., 2014; *Ward*, 2008].

A positive correlation between NTR_B and ammonium concentrations has been found at the Changjiang River inner plume [*Hsiao et al*., 2014], Hood Canal [*Horak et al*., 2013], and Sargasso Sea [*Newell et al*., 2013]. And the substrate concentrations in these regions were nM level, and the dominant nitrifier was *Archaea*. The half-saturation constant (k_m) values for nitrification in the Hood Canal and the Sargasso Sea (100 m) were 98 nmol L^{-1} and 65 ± 41 nmol L^{-1}, respectively [*Horak et al*., 2013; *Newell et al*., 2013]. Thus, under substrate limited condition, it is reasonable that NTR varied with ammonium concentrations in these regions. However, the ammonium concentrations in our study were orders of magnitude higher, suggesting substrate limitation of NTR was unlikely (although a positive correlation between NTR_B and ammonium concentrations was found in winter ($r = 0.83$, $p = 0.01$) (Figure 5c and Table S1b). Previous pure culture studies indicated the minimum concentration required for AOB was higher than 1 μmol L^{-1} at neutral pH [*Bollmann et al*., 2002] and the k_m value of AOA was much lower (133 nmol L^{-1}), and the substrate threshold for *Candidatus Nitrosopumilus maritimus*-SCM1 growth was even less than 10 nmol L^{-1} [*Martens-Habbena et al*., 2009]. Thus, the positive relationship for winter may attribute to the unsaturated substrate concentration (1.1–16.8 μmol L^{-1}) for AOB. Although we did not measure the abundance of AOA and AOB, the ammonium concentrations in autumn and summer were higher than 10 μmol L^{-1} (10 times higher than in winter), which were not limiting for AOA or AOB. Thus, no significant relation between NTR and ammonium concentration could be found in these two seasons.

In riverine and estuarine environments, salinity is an important and perhaps the main factor that regulates the distribution of nitrifier biomass and NTR [*Ward*, 2008]. A seaward decreasing pattern with high NTR values associated with low or intermediate salinity has been observed in many previous studies (e.g., the highest NTR levels in the Mississippi River (salinity of 7), the Atchafalaya River plume (salinity of 8) [*Pakulski et al*., 2000], Kochi backwaters (salinity of 20) [*Miranda et al*., 2008], and the Changjiang River plume (salinity of 29) [*Hsiao et al*., 2014]). However, in our study, salinity values varied in a very narrow range within a season due to limited freshwater influence; thus, NTR was not found to be correlated to salinity changes (Table S1).

Recent studies have indicated that decreasing water pH may inhibit NTR [e.g., *Beman et al*., 2011; *Kitidis et al*., 2011], while another studies found nagative correlations [e.g., *Fulweiler et al*., 2011]. Due to shallow depth and well vertical mixing, the pH variation within a season was insignificant (Table S1); thus, pH was not the controlling factor of NTR_B variations.

In summary, the main factor regulating NTR varied seasonally. In autumn, the NTR was varying only with TSS (Table S1a). In winter, as the TSS concentrations varied in a narrow range, ammonium concentration became the dominant factor in regulating the NTR (Table S1b). However, there was lack of correlation for NTR with any parameters in summer (Table S1c). When we put the three seasons of data together, we found that many parameters covaried (e.g., TSS covaried with temperature, salinity, pH, and NO_x^- concentration; Table S2). NTR may positively correlate with TSS, temperature, salinity, ammonium concentration, and NO_x^- concentration, and negatively correlate with pH (Table S2). A partial correlation analysis (holding the covarying parameters constant) was conducted to evaluate the influence of individual parameter on NTR. Results show that only the influences of TSS and temperature on NTR were statistically significant (Table S3). According to our observations, in addition to temperature, tidal energy may thus play a role in modulating NTR variations, via its influence on suspended particle abundances.

5. Conclusions and Implications

Through temperature manipulation experiments, a high degree of temperature dependence was observed for nitrification in a coastal system where the substrate was replete. Regardless of distinctive temperature and particulate concentrations among different seasons, nitrification exhibited consistent temperature dependence in all cases (including bulk, particle-associated, and free-living) with a consistent Q_{10} value of ~2.2. Ocean temperature will inevitably increase as the atmospheric CO_2 keeps rising. The strong temperature dependence of nitrification suggests that global warming would enhance nitrification in coastal regions where the substrate was replete. In the meantime, global warming may reduce dissolved oxygen concentration and increase stratification; consequently, the increasing nitrification may likely exacerbate coastal hypoxia when oxygen supply is further limited. As mentioned in section 1, acidification could be intensified also due to more proton release via nitrification of allochthonous ammonium.

On the other hand, our study also found that NTR is closely associated with particle concentration, which is influenced by rainfall, land use, dam construction in the watershed, and tidal/wave energy in the coastal zone. Interestingly, the optimum temperature for NTR_P was 5°C higher than that for the free-living organisms, although the mechanism remains unknown. Further studies regarding temperature effect on the size-fractioned NTR are needed to explore the mechanism and net particle effect on coastal nitrification.

Finally, high-temperature dependence and suspended particle reliance suggest that nitrification is very sensible to seasonal temperature change or global warming and to ocean dynamics (i.e., energy-induced resuspension). To better understand how the nitrification responds to multiple factors, more in situ nitrification investigations should be conducted in different environments with various levels of ammonium, pH, turbidity, and oxygen. Similar temperature manipulation experiments should be implemented to enable extrapolation of the temperature effects up to global scale. Meanwhile, studies of the temperature effect on nitrification-associated N_2O production are required to unravel the feedbacks of nitrification processes to global warming scenarios.

Acknowledgments
We sincerely thank Weijie Zhang for assisting with the summer experiment. Comments from Ting-Chang Hsu at Academia Sinica and from Bingzhang Chen at Xiamen University greatly improved this manuscript. We thank Xufeng Zheng from the Chinese Academy of Sciences for his help with the statistical analysis, and Tom Trull, MEL visiting scholar, for proof reading. This research was funded by the National Natural Science Foundation of China (NSFC U1305233 and 91328207), National Key Basic Research Program of China (973 Program 2014CB953702 and 2015CB954003), and MEL publication foundation (#melpublication 2017189). All the original data are presented in Tables 1, S4, and S5.

References

Baer, S. E., T. L. Connelly, R. E. Sipler, P. L. Yager, and D. A. Bronk (2014), Effect of temperature on rates of ammonium uptake and nitrification in the western coastal Arctic during winter, spring, and summer, *Global Biogeochem. Cycles*, *28*, 1455–1466, doi:10.1002/2013GB004765.

Beman, J. M., C. E. Chow, A. L. King, Y. Y. Feng, J. A. Fuhrman, A. Andersson, N. R. Bates, B. N. Popp, and D. A. Hutchins (2011), Global declines in oceanic nitrification rates as a consequence of ocean acidification, *Proc. Natl. Acad. Sci. U.S.A.*, *108*(1), 208–213, doi:10.1073/pnas.1011053108.

Beman, J. M., B. N. Popp, and S. E. Alford (2012), Quantification of ammonia oxidation rates and ammonia-oxidizing archaea and bacteria at high resolution in the Gulf of California and eastern tropical North Pacific Ocean, *Limnol. Oceanogr.*, *57*(3), 711–726, doi:10.4319/lo.2012.57.3.0711.

Bendschneider, K., and R. J. Robinson (1952), A new spectrophotometric method for the determination of nitrite in sea water, *J. Mar. Res.*, *11*, 87–96.

Berounsky, V. M., and S. W. Nixon (1990), Temperature and annual cycle of nitrification in waters of Narragansett Bay, *Limnol. Oceanogr.*, *35*(7), 1610–1617, doi:10.4319/lo.1990.35.7.1610.

Berounsky, V. M., and S. W. Nixon (1993), Rates of nitrification along an estuarine gradient in Narragansett Bay, *Estuaries*, *16*(4), 718–730, doi:10.2307/1352430.

Bollmann, A., M.-J. Bär-Gilissen, and H. J. Laanbroek (2002), Growth at low ammonium concentrations and starvation response as potential factors involved in niche differentiation among ammonia-oxidizing bacteria, *Appl. Environ. Microbiol.*, *68*(10), 4751–4757, doi:10.1128/AEM.68.10.4751-4757.2002.

Bouskill, N. J., J. Tang, W. J. Riley, and E. L. Brodie (2012), Trait-based representation of biological nitrification: Model development, testing, and predicted community composition, *Front. Microbiol.*, *3*, 364, doi:10.3389/fmicb.2012.00364.

Braman, R. S., and S. A. Hendrix (1989), Nanogram nitrite and nitrate determination in environmental and biological materials by vanadium (III) reduction with chemiluminescence detection, *Anal. Chem.*, *61*(24), 2715–2718, doi:10.1021/ac00199a007.

Brion, N., G. Billen, L. Guézennec, and A. Ficht (2000), Distribution of nitrifying activity in the Seine River (France) from Paris to the estuary, *Estuaries*, *23*(5), 669–682, doi:10.2307/1352893.

Brzostek, E. R., and A. C. Finzi (2012), Seasonal variation in the temperature sensitivity of proteolytic enzyme activity in temperate forest soils, *J. Geophys. Res.*, *117*, G01018, doi:10.1029/2011JG001688.

Casciotti, K., D. Sigman, M. G. Hastings, J. Böhlke, and A. Hilkert (2002), Measurement of the oxygen isotopic composition of nitrate in seawater and freshwater using the denitrifier method, *Anal. Chem.*, *74*(19), 4905–4912, doi:10.1021/ac020113w.

Collins, M., et al. (2013), Long-term climate change: Projections, commitments and irreversibility, in *Climate Change 2013: The Physical Science Basis. Contribution of Working Group I to the Fifth Assessment Report of the Intergovernmental Panel on Climate Change*, edited by B. F. Christopher et al., pp. 1029–1136, Cambridge Univ., New York.

Dai, M., L. Wang, X. Guo, W. Zhai, Q. Li, B. He, and S.-J. Kao (2008), Nitrification and inorganic nitrogen distribution in a large perturbed river/estuarine system: The Pearl River estuary, China, *Biogeosciences*, *5*(5), 1227–1244, doi:10.5194/bg-5-1227-2008.

Dai, Z., J. Du, X. Zhang, N. Su, and J. Li (2010), Variation of riverine material loads and environmental consequences on the Changjiang (Yangtze) estuary in recent decades (1955−2008), *Environ. Sci. Technol.*, *45*(1), 223–227, doi:10.1021/es103026a.

Damashek, J., K. L. Casciotti, and C. A. Francis (2016), Variable nitrification rates across environmental gradients in turbid, nutrient-rich estuary waters of San Francisco Bay, *Estuar. Coasts*, *39*(4), 1050–1071, doi:10.1007/s12237-016-0071-7.

Deser, C., A. S. Phillips, and M. A. Alexander (2010), Twentieth century tropical sea surface temperature trends revisited, *Geophys. Res. Lett.*, *37*, L10701, doi:10.1029/2010GL043321.

Fulweiler, R. W., H. E. Emery, E. M. Heiss, and V. M. Berounsky (2011), Assessing the role of pH in determining water column nitrification rates in a coastal system, *Estuar Coasts*, *34*(6), 1095–1102, doi:10.1007/s12237-011-9432-4.

Füssel, J., P. Lam, G. Lavik, M. M. Jensen, M. Holtappels, M. Günter, and M. M. Kuypers (2012), Nitrite oxidation in the Namibian oxygen minimum zone, *ISME J.*, *6*(6), 1200–1209, doi:10.1038/ismej.2011.178.

Feng, Y., C. E. Hare, K. Leblanc, J. M. Rose, Y. Zhang, G. R. DiTullio, P. Lee, S. Wilhelm, J. M. Rowe, and J. Sun (2009), The effects of increased p_{CO2} and temperature on the North Atlantic spring bloom: I. The phytoplankton community and biogeochemical response, *Mar. Ecol. Prog. Ser.*, *388*, 13–25, doi:10.3354/meps08133.

Ganesh, S., L. A. Bristow, M. Larsen, N. Sarode, B. Thamdrup, and F. J. Stewart (2015), Size-fraction partitioning of community gene transcription and nitrogen metabolism in a marine oxygen minimum zone, *ISME J.*, *9*(12), 2682–2696, doi:10.1038/ismej.2015.44.

García-Serna, J., E. García-Merino, and M. J. Cocero (2013), Large-scale patterns of river inputs in southwestern Europe: Seasonal and interannual variations and potential eutrophication effects at the coastal zone, *Biogeochemistry*, *113*(1–3), 481–505, doi:10.1016/j.supflu.2006.12.019.

Groeneweg, J., B. Sellner, and W. Tappe (1994), Ammonia oxidation in nitrosomonas at NH3 concentrations near km: Effects of pH and temperature, *Water Res.*, *28*(12), 2561–2566, doi:10.1016/0043-1354(94)90074-4.

Gruber, N., and J. N. Galloway (2008), An Earth-system perspective of the global nitrogen cycle, *Nature*, *451*(7176), 293–296, doi:10.1038/nature06592.

Grundle, D. S., and S. K. Juniper (2011), Nitrification from the lower euphotic zone to the sub-oxic waters of a highly productive British Columbia fjord, *Mar. Chem.*, *126*(1), 173–181, doi:10.1016/j.marchem.2011.06.001.

Heiss, E. M., and R. W. Fulweiler (2016), Coastal water column ammonium and nitrite oxidation are decoupled in summer, *Estuar. Coast. Shelf Sci.*, *178*, 110–119, doi:10.1016/j.ecss.2016.06.002.

Horak, R. E. A., W. Qin, A. J. Schauer, E. V. Armbrust, A. E. Ingalls, J. W. Moffett, D. A. Stahl, and A. H. Devol (2013), Ammonia oxidation kinetics and temperature sensitivity of a natural marine community dominated by *Archaea*, *ISME J.*, *7*(10), 2023–2033, doi:10.1038/ismej.2013.75.

Hsiao, S.-Y., T.-C. Hsu, J.-w. Liu, X. Xie, Y. Zhang, J. Lin, H. Wang, J.-Y. Yang, S.-C. Hsu, and M. Dai (2014), Nitrification and its oxygen consumption along the turbid Chang Jiang River plume, *Biogeosciences*, *11*(7), 2083–2098, doi:10.5194/bg-11-2083-2014.

Hu, X., and W. J. Cai (2011), An assessment of ocean margin anaerobic processes on oceanic alkalinity budget, *Global Biogeochem. Cycles*, *25*, GB3003, doi:10.1029/2010GB003859.

Isnansetyo, A., S. Getsu, M. Seguchi, and M. Koriyama (2014), Independent effects of temperature, salinity, ammonium concentration and pH on nitrification rate of the Ariake seawater above mud sediment, *Hayati J. Biosci.*, *21*(1), 21–30, doi:10.4308/hjb.21.1.21.

Johnson, M. T., P. S. Liss, T. G. Bell, T. J. Lesworth, A. R. Baker, A. J. Hind, T. D. Jickells, K. F. Biswas, E. M. S. Woodward, and S. W. Gibb (2008), Field observations of the ocean-atmosphere exchange of ammonia: Fundamental importance of temperature as revealed by a comparison of high and low latitudes, *Global Biogeochem. Cycles*, *22*, GB1019, doi:10.1029/2007GB003039.

Kim, I.-N., K. Lee, N. Gruber, D. M. Karl, J. L. Bullister, S. Yang, and T.-W. Kim (2014), Increasing anthropogenic nitrogen in the North Pacific Ocean, *Science*, *346*(6213), 1102–1106, doi:10.1126/science.1258396.

Kitidis, V., B. Laverock, L. C. McNeill, A. Beesley, D. Cummings, K. Tait, M. A. Osborn, and S. Widdicombe (2011), Impact of ocean acidification on benthic and water column ammonia oxidation, *Geophys. Res. Lett.*, *38*, L21603, doi:10.1029/2011GL049095.

Koops, H. P., U. Purkhold, A. P. Röser, G. Timmermann, M. Wagner, and M. Wagner (2006), Lithotrophic ammonia-oxidizing bacteria, in *The Prokaryotes*, edited by M. Dworkin et al., pp. 778–811, Springer, New York.

Liltved, H., and S. Cripps (1999), Removal of particle-associated bacteria by prefiltration and ultraviolet irradiation, *Aquac. Res.*, *30*(6), 445–450, doi:10.1046/j.1365-2109.1999.00349.x.

Lipschultz, F., S. C. Wofsy, and L. E. Fox (1986), Nitrogen metabolism of the eutrophic Delaware River ecosystem, *Limnol. Oceanogr.*, *31*(4), 701–716, doi:10.4319/lo.1986.31.4.0701.

Martens-Habbena, W., P. M. Berube, H. Urakawa, J. R. de La Torre, and D. A. Stahl (2009), Ammonia oxidation kinetics determine niche separation of nitrifying *Archaea* and bacteria, *Nature*, *461*(7266), 976–979, doi:10.1038/nature08465.

Miranda, J., K. Balachandran, R. Ramesh, and M. Wafar (2008), Nitrification in Kochi backwaters, *Estuar. Coast. Shelf Sci.*, *78*(2), 291–300, doi:10.1016/j.ecss.2007.12.004.

Moeseneder, M. M., C. Winter, and G. J. Herndl (2001), Horizontal and vertical complexity of attached and free-living bacteria of the eastern Mediterranean Sea, determined by 16S rDNA and 16S rRNA fingerprints, *Limnol. Oceanogr.*, *46*(1), 95–107, doi:10.4319/lo.2001.46.1.0095.

Newell, S. E., A. R. Babbin, A. Jayakumar, and B. B. Ward (2011), Ammonia oxidation rates and nitrification in the Arabian Sea, *Global Biogeochem. Cycles*, *25*, GB4016, doi:10.1029/2010GB003940.

Newell, S. E., S. E. Fawcett, and B. B. Ward (2013), Depth distribution of ammonia oxidation rates and ammonia-oxidizer community composition in the Sargasso Sea, *Limnol. Oceanogr.*, *58*(4), 1491–1500, doi:10.4319/lo.2013.58.4.1491.

Orsi, W. D., J. M. Smith, H. M. Wilcox, J. E. Swalwell, P. Carini, A. Z. Worden, and A. E. Santoro (2015), Ecophysiology of uncultivated marine euryarchaea is linked to particulate organic matter, *ISME J.*, *9*(8), 1747–1763, doi:10.1038/ismej.2014.260.

Pai, S.-C., Y.-J. Tsau, and T.-I. Yang (2001), pH and buffering capacity problems involved in the determination of ammonia in saline water using the indophenol blue spectrophotometric method, *Anal. Chim. Acta*, *434*(2), 209–216, doi:10.1016/S0003-2670(01)00851-0.

Pakulski, J., R. Benner, T. Whitledge, R. Amon, B. Eadie, L. Cifuentes, J. Ammerman, and D. Stockwell (2000), Microbial metabolism and nutrient cycling in the Mississippi and Atchafalaya River plumes, *Estuar. Coast. Shelf Sci.*, *50*(2), 173–184, doi:10.1006/ecss.1999.0561.

Peng, X., C. A. Fuchsman, A. Jayakumar, S. Oleynik, W. Martens-Habbena, A. H. Devol, and B. B. Ward (2015), Ammonia and nitrite oxidation in the eastern tropical North Pacific, *Global Biogeochem. Cycles*, *29*, 2034–2049, doi:10.1002/2015GB005278.

Peng, X., C. A. Fuchsman, A. Jayakumar, M. J. Warner, A. H. Devol, and B. B. Ward (2016), Revisiting nitrification in the eastern tropical South Pacific: A focus on controls, *J. Geophys. Res. Oceans*, *121*, 1667–1684, doi:10.1002/2015JC011455.

Qin, W., S. A. Amin, W. Martens-Habbena, C. B. Walker, H. Urakawa, A. H. Devol, A. E. Ingalls, J. W. Moffett, E. V. Armbrust, and D. A. Stahl (2014), Marine ammonia-oxidizing archaeal isolates display obligate mixotrophy and wide ecotypic variation, *Proc. Natl. Acad. Sci. U.S.A.*, *111*(34), 12504–12509, doi:10.1073/pnas.1324115111.

Rockström, J., W. Steffen, K. Noone, A. Persson, C. F. Rd, E. F. Lambin, T. M. Lenton, M. Scheffer, C. Folke, and H. J. Schellnhuber (2009), A safe operating space for humanity, *Nature*, *461*(7263), 472–475, doi:10.1038/461472a.

Santoro, A. E., C. Buchwald, M. R. McIlvin, and K. L. Casciotti (2011), Isotopic signature of N_2O produced by marine ammonia-oxidizing archaea, *Science*, *333*(6047), 1282–1285, doi:10.1126/science.1208239.

Shiozaki, T., K. Furuya, T. Kodama, and S. Takeda (2009), Contribution of N_2 fixation to new production in the western North Pacific Ocean along 155°E, *Mar. Ecol. Prog. Ser.*, *377*, 19–32, doi:10.3354/meps07837.

Sigman, D., K. Casciotti, M. Andreani, C. Barford, M. Galanter, and J. Böhlke (2001), A bacterial method for the nitrogen isotopic analysis of nitrate in seawater and freshwater, *Anal. Chem.*, *73*(17), 4145–4153, doi:10.1021/ac010088e.

Spieck, E., and E. Bock (2005), The lithoautotrophic nitrite-oxidizing bacteria, in *Bergey's Manual of Systematic Bacteriology*, edited by G. M. Garrity, pp. 149–153, Springer, New York.

Stratton, F. E., and P. L. McCarty (1967), Prediction of nitrification effects of the dissolved oxygen balance of streams, *Environ. Sci. Technol.*, *1*(5), 405–410, doi:10.1021/es60005a003.

Sudarno, U., J. Winter, and C. Gallert (2011), Effect of varying salinity, temperature, ammonia and nitrous acid concentrations on nitrification of saline wastewater in fixed-bed reactors, *Bioresour. Technol.*, *102*(10), 5665–5673, doi:10.1016/j.biortech.2011.02.078.

Suzuki, I., U. Dular, and S. Kwok (1974), Ammonia or ammonium ion as substrate for oxidation by *Nitrosomonas europaea* cells and extracts, *J. Bacteriol.*, *120*(1), 556–558.

Tourna, M., T. E. Freitag, G. W. Nicol, and J. I. Prosser (2008), Growth, activity and temperature responses of ammonia-oxidizing archaea and bacteria in soil microcosms, *Environ. Microbiol.*, *10*(5), 1357–1364, doi:10.1111/j.1462-2920.2007.01563.x.

Wang, H., Z. Shen, X. Guo, J. Niu, and B. Kang (2010), Ammonia adsorption and nitritation in sediments derived from the Three Gorges Reservoir, China, *Environ. Earth Sci.*, *60*(8), 1653–1660, doi:10.1007/s12665-009-0299-7.

Ward, B. B. (1987), Kinetic studies on ammonia and methane oxidation by *Nitrosococcus oceanus*, *Arch. Microbiol.*, *147*(2), 126–133, doi:10.1007/BF00415273.

Ward, B. B. (2005), Temporal variability in nitrification rates and related biogeochemical factors in Monterey Bay, California, USA, *Mar. Ecol. Prog. Ser.*, *292*(97), 97, doi:10.3354/meps292097.

Ward, B. B. (2008), Nitrification in marine systems, in *Nitrogen in the Marine Environment*, edited by D. G. Capone et al., pp. 199–261, Elsevier, Netherlands.

Ward, B. (2011), Measurement and distribution of nitrification rates in the oceans, in *Methods Enzymol*, edited by M. G. Klotz, pp. 307–323, Elsevier, Burlington, Canada.

Watson, S. W., F. W. Valois, and J. B. Waterbury (1981), The family nitrobacteraceae, in *The Prokaryotes: A Handbook on Habitats, Isolation and Identification of Bacteria*, edited by M. P. Starr et al., pp. 1005–1022, Springer, New York.

Wong, G., G. Gong, K. Liu, and S. Pai (1998), Excess Nitrate' in the East China Sea, Estuar, *Coast. Shelf Sci.*, *46*(3), 411–418, doi:10.1006/ecss.1997.0287.

Wu, Y., X. Ke, M. Hernández, B. Wang, M. G. Dumont, Z. Jia, and R. Conrad (2013), Autotrophic growth of bacterial and archaeal ammonia oxidizers in freshwater sediment microcosms incubated at different temperatures, *Appl. Environ. Microbiol.*, *79*(9), 3076–3084, doi:10.1128/AEM.00061-13.

Xia, X., Z. Yang, and X. Zhang (2009), Effect of suspended-sediment concentration on nitrification in river water: Importance of suspended sediment−water interface, *Environ. Sci. Technol.*, *43*(10), 3681–3687, doi:10.1021/es8036675.

Xu, M. N., Y. Wu, L. W. Zheng, Z. Zheng, H. Zhao, E. A. Laws, and S.-J. Kao (2017), Quantification of multiple simultaneously occurring nitrogen flows in the euphotic ocean, *Biogeosciences*, *14*(4), 1021, doi:10.5194/bg-14-1021-2017.

Yan, X., W. Zhai, H. Hong, Y. Li, W. Guo, and X. Huang (2012), Distribution, fluxes and decadal changes of nutrients in the Jiulong River estuary, Southwest Taiwan Strait, *Chin. Sci. Bull.*, *57*(18), 2307–2318, doi:10.1007/s11434-012-5084-4.

Yang, S., and N. Gruber (2016), The anthropogenic perturbation of the marine nitrogen cycle by atmospheric deposition: Nitrogen cycle feedbacks and the ^{15}N Haber-Bosch effect, *Global Biogeochem. Cycles*, *30*, 1418–1440, doi:10.1002/2016GB005421.

Zhang, Y., X. Xie, N. Jiao, S.-Y. Hsiao, and S.-J. Kao (2014), Diversity and distribution of amoA-type nitrifying and nirS-type denitrifying microbial communities in the Yangtze River estuary, *Biogeosciences*, *11*(8), 2131–2145, doi:10.5194/bg-11-2131-2014.